AD-A172 022   LUMINESCENT CHARACTERISTICS STUDY OF MATHER-TYPE DENSE   1/1
PLASMA FOCUS AND A..(U) ILLINOIS UNIV AT URBANA CHARGED
PARTICLE RESEARCH LAB K K KIM JUN 86 CPRL-2-86
UNCLASSIFIED   AFOSR-TR-86-0688 AFOSR-84-0138   F/G 20/5   NL

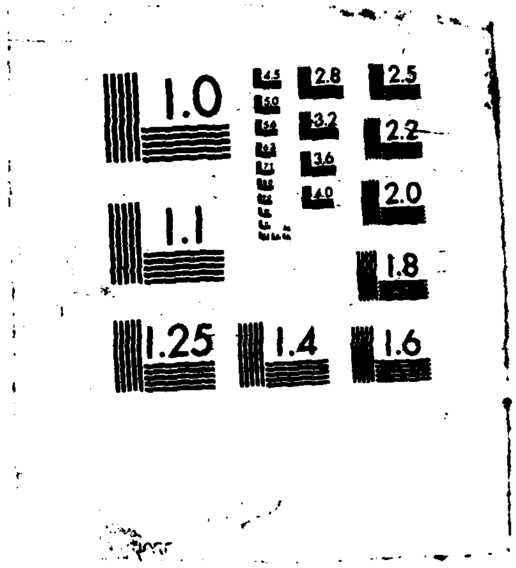
1.0
4.5
5.0
5.6
6.3
7.1
8.0
2.8
3.2
3.6
4.0
2.5
2.2
2.0
1.1
1.8
1.25
1.4
1.6

(2)

AFOSR-TR- 86-0688

CHARGED PARTICLE RESEARCH LABORATORY REPORT NO. 2-86

AD-A172 022

LUMINESCENT CHARACTERISTICS STUDY OF MATHER-TYPE DENSE PLASMA FOCUS AND APPLICATIONS TO SHORT-WAVELENGTH OPTICAL PUMPING

Final Technical Report prepared for AFOSR

by

KYEKYOON (KEVIN) KIM

CHARGED PARTICLE RESEARCH LABORATORY
DEPARTMENT OF ELECTRICAL AND COMPUTER ENGINEERING
UNIVERSITY OF ILLINOIS
URBANA, ILLINOIS 61801

June 1986

Research Sponsored partly by

THE AIR FORCE OFFICE OF SCIENTIFIC RESEARCH
UNITED STATES AIR FORCE

Under Grant No. AFOSR-84-0138

and by

THE RESEARCH BOARD AND THE PHYSICAL ELECTRONICS
AFFILIATED PROGRAM OF THE UNIVERSITY OF ILLINOIS

UNCLASSIFIED
SECURITY CLASSIFICATION OF THIS PAGE

REPORT DOCUMENTATION PAGE

1a. REPORT SECURITY CLASSIFICATION UNCLASSIFIED	1b. RESTRICTIVE MARKINGS
2a. SECURITY CLASSIFICATION AUTHORITY	3. DISTRIBUTION/AVAILABILITY OF REPORT Approved for public release; Distribution unlimited
2b. DECLASSIFICATION / DOWNGRADING SCHEDULE	
4. PERFORMING ORGANIZATION REPORT NUMBER(S) 2-86	5. MONITORING ORGANIZATION REPORT NUMBER(S) AFOSR-TR- 86-0688
6a. NAME OF PERFORMING ORGANIZATION University of Illinois — 6b. OFFICE SYMBOL (If applicable)	7a. NAME OF MONITORING ORGANIZATION AFOSR/NP
6c. ADDRESS (City, State, and ZIP Code) Urbana, IL 61801	7b. ADDRESS (City, State, and ZIP Code) Building 410 Bolling AFB DC 20332-6448
8a. NAME OF FUNDING/SPONSORING ORGANIZATION AFOSR — 8b. OFFICE SYMBOL (If applicable) NP	9. PROCUREMENT INSTRUMENT IDENTIFICATION NUMBER AFOSR 84-0138
8c. ADDRESS (City, State, and ZIP Code) Building 410 Bolling AFB DC 20332-6448	10. SOURCE OF FUNDING NUMBERS PROGRAM ELEMENT NO. 61102F; PROJECT NO. 2301; TASK NO. K1; WORK UNIT ACCESSION NO.

11. TITLE (Include Security Classification)
"LUMINESCENT CHARACTERISTICS STUDY OF MATHER-TYPE DENSE PLASMA FOCUS AND APPLICATIONS TO SHORT-WAVELENGTH OPTICAL PUMPING"

12. PERSONAL AUTHOR(S)
Dr Kyekyoon (Kevin) Kim

13a. TYPE OF REPORT	13b. TIME COVERED	14. DATE OF REPORT (Year, Month, Day)	15. PAGE COUNT
FINAL	FROM 01 May 84 TO 30 Sep 85	June 1986	35

16. SUPPLEMENTARY NOTATION

17. COSATI CODES			18. SUBJECT TERMS (Continue on reverse if necessary and identify by block number)
FIELD	GROUP	SUB-GROUP	

19. ABSTRACT (Continue on reverse if necessary and identify by block number) A Mather-type dense plasma focus (MDPF) system was designed, built, and tested specifically to study its luminescent characteristics and to assess its potential as a new light source of high-energy, short-wavelength lasers. The luminescence study of MDPF showed that the conversion efficiency from the electrical input to the optical output energies is at least 50%, up to the time the plasma compression is complete. Using the system, for the first time as an optical pump, laser activities were successfully obtained from a variety of liquid organic dyes. Diagnostic capabilities included an optical multichannel analyzer system complete with a computer control, a nitrogen-pumped tunable dye laser system, a high-speed streak/framing camera, a digital laser energy meter, voltage and current probes, and a computer-based data acquisition system.

20. DISTRIBUTION/AVAILABILITY OF ABSTRACT ☐ UNCLASSIFIED/UNLIMITED ☒ SAME AS RPT. ☐ DTIC USERS	21. ABSTRACT SECURITY CLASSIFICATION Unclassified
22a. NAME OF RESPONSIBLE INDIVIDUAL Dr Howard R. Schlossberg	22b. TELEPHONE (Include Area Code) 202/767-4906 — 22c. OFFICE SYMBOL NP

DD FORM 1473, 84 MAR — 83 APR edition may be used until exhausted. All other editions are obsolete.

SECURITY CLASSIFICATION OF THIS PAGE
UNCLASSIFIED

UILU-ENG-86-2551

CHARGED PARTICLE RESEARCH LABORATORY REPORT NO. 2-86

LUMINESCENT CHARACTERISTICS STUDY OF MATHER-TYPE DENSE PLASMA FOCUS AND APPLICATIONS TO SHORT-WAVELENGTH OPTICAL PUMPING

Final Technical Report prepared for AFOSR

by

KYEKYOON (KEVIN) KIM

CHARGED PARTICLE RESEARCH LABORATORY
DEPARTMENT OF ELECTRICAL AND COMPUTER ENGINEERING
UNIVERSITY OF ILLINOIS
URBANA, ILLINOIS 61801

June 1986

Research Sponsored partly by

THE AIR FORCE OFFICE OF SCIENTIFIC RESEARCH
UNITED STATES AIR FORCE

Under Grant No. AFOSR-84-0138

and by

THE RESEARCH BOARD AND THE PHYSICAL ELECTRONICS
AFFILIATED PROGRAM OF THE UNIVERSITY OF ILLINOIS

TABLE OF CONTENTS

ABSTRACT 1

I. SUMMARY 2

A. Technical Objective 4

B. Status of Research 6

C. List of Professional Personnel Involved 8

D. A Cumulative Chronological List of Written Publications 8

E. Interactions (Coupling Activities) 8

II. EXPERIMENTAL DEVELOPMENT AND RESULTS 9

A. Justification 9

B. Experimental Efforts - Achievements and Efforts 10

C. References 26

III. CONCLUSIONS 28

ABSTRACT

A Mather-type dense plasma focus (MDPF) system was designed, built, and tested specifically to study its luminescent characteristics and to assess its potential as a new light source for high-energy, short-wavelength lasers. The luminescence study of MDPF showed that the conversion efficiency from the electrical input to the optical output energies is at least 50%, up to the time the plasma compression is complete. Using the system, for the first time as an optical pump, laser activities were successfully obtained from a variety of liquid organic dyes. Diagnostic capabilities included an optical multichannel analyzer system complete with a computer control, a nitrogen-pumped tunable dye laser system, a high-speed streak/framing camera, a digital laser energy meter, voltage and current probes, and a computer-based data acquisition system.

I. SUMMARY

This report is a final documentation of research performed on the luminescent characteristics study of a Mather-type dense plasma focus (MDPF) and the evaluation of its potential as a new short-wavelength optical pump. One of the principal goals of this research was to develop an intense light source which can be fired repeatedly, which has a long lifetime, and which, most of all, has a narrow spectral distribution overlapping the absorption bands ($\leq$ 200 nm) of the many UV and blue-green laser media.

During the duration of the program supported by AFOSR (Contract No. AFOSR-84-0138), an MDPF system was designed, built, and tested, specifically to study its luminescent characteristics and to assess its potential as a new excitation light source for lasers. The highlights of these research activities were as follows: first, preliminary results were obtained for the MDPF plasma indicating that conversion efficiency from the electrical input to the optical output energies is very high. Specifically, it was found that the conversion efficiency in the spectral region from the vacuum ultraviolet to infrared, up to the time the plasma compression is complete, is at least 50%, with approximately 80% of the emitted radiation in the wavelengths less than 300 nm. Second, an MDPF machine was operated, for the first time, as an optical pump to successfully create laser activities from a variety of liquid organic dyes. By employing a small dye cuvette of 2-cm^3 volume and utilizing less than 5% of the total available MDPF light, a laser output energy of approximately 0.7 J was achieved for a 1-μs laser pulse. This MDPF-based laser system featured a cylindrical plasma chamber which formed an optically active plasma focus at the top of the chamber and a laser cavity complete with a custom-made light reflector which was designed to focus the plasma light for the laser optical pumping. Diagnostic capabilities included an optical spectrometric multichannel analyzer system with a computer control, a

nitrogen-pumped tunable dye laser system, a digital laser energy meter, voltage and current probes, and a computer-based data acquisition system.

A. Technical Objectives

Since one of the major goals of this work was to develop an intense light source which can be fired repeatedly, which has a long lifetime, and which most of all, has a narrow spectral distribution overlapping the absorption bands (200 nm) of the many UV and blue-green laser media, the principal research effort was in the areas outlined below.

1. Luminescence Characteristics Study of MDPF

There were two primary goals in the experimental phase of this project. The first goal was a complete characterization and understanding of the MDPF luminescence to provide a clue for the design of an optimal system which will efficiently serve the specific optical pumping needs. The second goal was to come up with a specific design which will be most suitable for pumping such laser media as XeF_2, I_2, and CN requiring fast risetimes and short pumping wavelengths.

2. Lasing Study with MDPF

With improvements on the existing proof-of-principle MDPF-based laser system, the lasing study was to be carried out, first with the blue-green and UV dyes and then with a wide range of candidate lasing media requiring short pumping wavelengths. This study was mainly for optimizing the laser cavity and other optical arrangements and for compiling a preliminary shopping list of the UV and blue-green lasers which may be optically pumped by the MDPF.

3. Diagnostics Development

Diagnostics required for accurately measuring the UV and VUV emissions of the MDPF were to be developed as a means for extending the capabilities of the existing spectroscopic equipment. Also, to improve as well as speed up some of the existing diagnostics, an effort was to be directed toward digitizing and processing the experimental results by using a few essential low-cost components, most of which were already available. This was intended to be a preparation for the eventual conversion of the existing data acquisition system to one that is computer-based and therefore most efficient for the data storage and processing.

B. Status of Research

The highlights of the research achievements were as follows:

1. A Mather-type dense plasma focus (MDPF) system which can easily be coupled to a laser cavity for lasing experiments was designed, constructed and operated.

2. Diagnostics that are suitable for observing the dynamics of the MDPF plasma and especially its luminescent characteristics were developed and implemented.

3. Detailed measurements of the temporal and spectral characteristics of the MDPF plasma were made. Some of the important conclusions were:

   a. MDPF is an efficient source of VUV-to-visible radiation for short-wavelength laser pumping and UV microlithography.

   b. The dominant radiation mechanism in MDPF is the electron bombardment of the anode. Proper design of the anode cap is, therefore, vital in optimizing the radiated output. Results indicated that a smooth concave depression in a high-Z material, such as tungsten or tantalum, will produce the greatest optical power output.

   c. In contrast to the earlier belief that the MDPF-radiated output could be tuned specifically to a desired spectral band, the data with different fill gases and pressures, anode materials, and operation energies indicated that only a minimal selectivity in spectral output is possible.

d. Best luminescent characteristics were obtained with a properly designed anode constructed out of high-Z material and 2-3 Torr hydrogen gas. The resultant spectrum was a very broad continuum extending from deep in the VUV to approximately 550 nm.

4. For the first time, MDPF was successfully operated at 5 kV. This success was largely due to the improved breakdown performance effected by addition of a knife edge to the cathode structure. Low-voltage MDPF operation will permit development of a compact, reliable solid-state switched MDPF capable of high repetition rates.

5. For the first time, successful operation of an MDPF as an optical pump source for lasers was achieved. For these proof-of-principle experiments a variety of organic liquid dyes was used. Experiments with energy scaling indicated that a *superlinear* relationship between increases in electrical input energy and the resultant optical or laser output energies.

6. Preliminary data indicated that the MDPF plasma can provide an ideal source of high-intensity radiation for soft x-ray and VUV microlithography. With adoption of MgF_2 optics the intense VUV radiation from MDPF should allow for generation of micron- and submicron-sized geometries on integrated circuits.

C. List of Professional Personnel Involved

Kyekyoon (Kevin) Kim, Principal Investigator, Professor

James J. Fanning, Graduate Research Assistant, a Ph.D. candidate; currently with Sandia Lab, Albuquerque, New Mexico

Kurt W. Gleichman, Graduate Research Assistant, an M.S. candidate; currently with Environmental Research Institute of Michigan, Ann Arbor, Michigan

D. A Cumulative Chronological List of Written Publications

J.J. Fanning and K. Kim, "Performance evaluation of a Mather-type dense plasma focus as a new excitation light source for pumping rhodamine-6G dye laser," manuscript in preparation for submission to J. Appl. Phys. (1986).

E. Interactions (Coupling Activities)

J.J. Fanning and K. Kim, "Performance of high-density high-temperature plasmas for short-wavelength optical pumping of lasers," Proc. Conference on Lasers and Electro-Optics, May 21-24, 1985, Baltimore, MD.

II. EXPERIMENTAL DEVELOPMENT AND RESULTS

The key elements of the program were the spectral and temporal characterizations of the MDPF luminescence and its development and application as a short-wavelength optical pump. The experimental facility featured an MDPF machine, a laser cavity specially designed to utilize the MDPF luminescence as the optical pump, and the diagnostics capable of monitoring both the electrical and optical signatures of the MDPF plasma which are essential to the characterization of the system performance. The results obtained were very encouraging and provided a convincing basis for further investigation.

A. Justification

Xenon flashlamps, which are presently the most commonly adopted optical pump sources, can deliver an intense light of a broad spectrum. However, when the required optical pump wavelengths fall below 200 nm, which is often the case with most gas media lasing at wavelengths between 200 nm and 500 nm, their efficiency (and, therefore, their utility) becomes so insignificant that they can no longer serve as a useful optical pump. To circumvent this drawback, a few alternative short-wavelength light sources have been tested, the most successful being the exploding wire plasma discharge of which the Russians have been the predominant investigators. An obvious drawback to this exploding-wire approach is that it is limited to a single-shot operation. Other optical pumping sources tested thus far mainly consist of high-temperature high-density plasmas of a few different configurations,[1-22] which are not effective either because of the low-level emission in the short wavelengths or the configurational inadequacy as a laser optical pump.

The MDPF device,[23,24], however, appears to defy all of these drawbacks

and, therefore, qualifies as a promising candidate for a short-wavelength optical pump. This optimism was extensively substantiated by the preliminary results obtained at the outset of the program,[25] which included the systematic spectrometric study of the MDPF luminescence and the first successful operation of MDPF as a laser optical pump in more than 20 years after its advent as a device for forming high-density, high-temperature plasmas.[26] Continuation of the program was essential not only to fully understand the luminescent behavior of the MDPF plasma but to further explore its capabilities and limitations as a new short-wavelength optical pump.

B. Experimental Efforts - Achievements and Efforts

A concerted effort was expended to characterize the luminescent behavior of a specially designed MDPF system and to assess its application potential as a new short-wavelength optical pump. Specifically, work was performed in the following four categories:

1. Design, construction, and operation of an MDPF system which can easily be coupled to a laser cavity for lasing experiments.

2. Development and implementation of diagnostics that are suitable for observing the dynamics of the MDPF plasma and especially its luminescent characteristics.

3. Measurement of the temporal and spectral characteristics of the MDPF plasma.

4. Lasing experiments using the MDPF luminescence as the optical pump.

Shown in Figs. 1 and 2 are the schematics illustrating the basic MDPF machine, the add-on laser cavity, the principal diagnostics, and the computer-based data acquisition system. As the figures indicate, the backbone of the MDPF machine is a gas-filled cylindrical chamber containing a pair of circularly symmetric metal electrodes separated at the breech by an insulator-vacuum seal. The cylinder is open at the muzzle for the emergence of plasma. A high-voltage, high-current power supply (in the present work, a capacitor bank) is connected across the electrodes at the breech, and the current is dumped into the system using a fast switch. The initial breakdown occurs at the breech along the surface of the insulator and the resulting discharge current sheet is accelerated, by the J x B force, toward the muzzle. At the end of the electrode, the plasma sheet symmetrically collapses toward the center axis, thus forming a very dense plasma focus.

To closely monitor the temporal and spectrometric characteristics of the MDPF plasma, which are essential to the development of MDPF as an efficient optical pump, a variety of diagnostics has been installed and is shown in Figs. 1 and 2. The Rogowski coil shown at the bottom of Fig. 1 monitors the temporal variations of the plasma current. The pump-light detector diode shown at the top of Fig. 1 measures the spectrally integrated optical output of the MDPF plasma and provides a quick glance at the temporal behavior of the plasma luminescence. To determine the luminescent output that lies in the specific spectral regions, a combination of photomultiplier tubes and bandpass filters is used. In this way, the optical power outputs in the range of 115-165 nm, 200-300 nm, 300-500 nm, and 500-930 nm were, respectively, determined. These particular diagnostics are immensely improved when an Optical Spectrometric Multichannel Analyzer (OSMA) system is implemented. This OSMA system consists of an IRY-700 high-speed gated intensified detector, FG-100 programmable high voltage pulser, and ST-110 OSMA controller and computer interface. The diagnostics package also includes a Jarrell-Ash brand

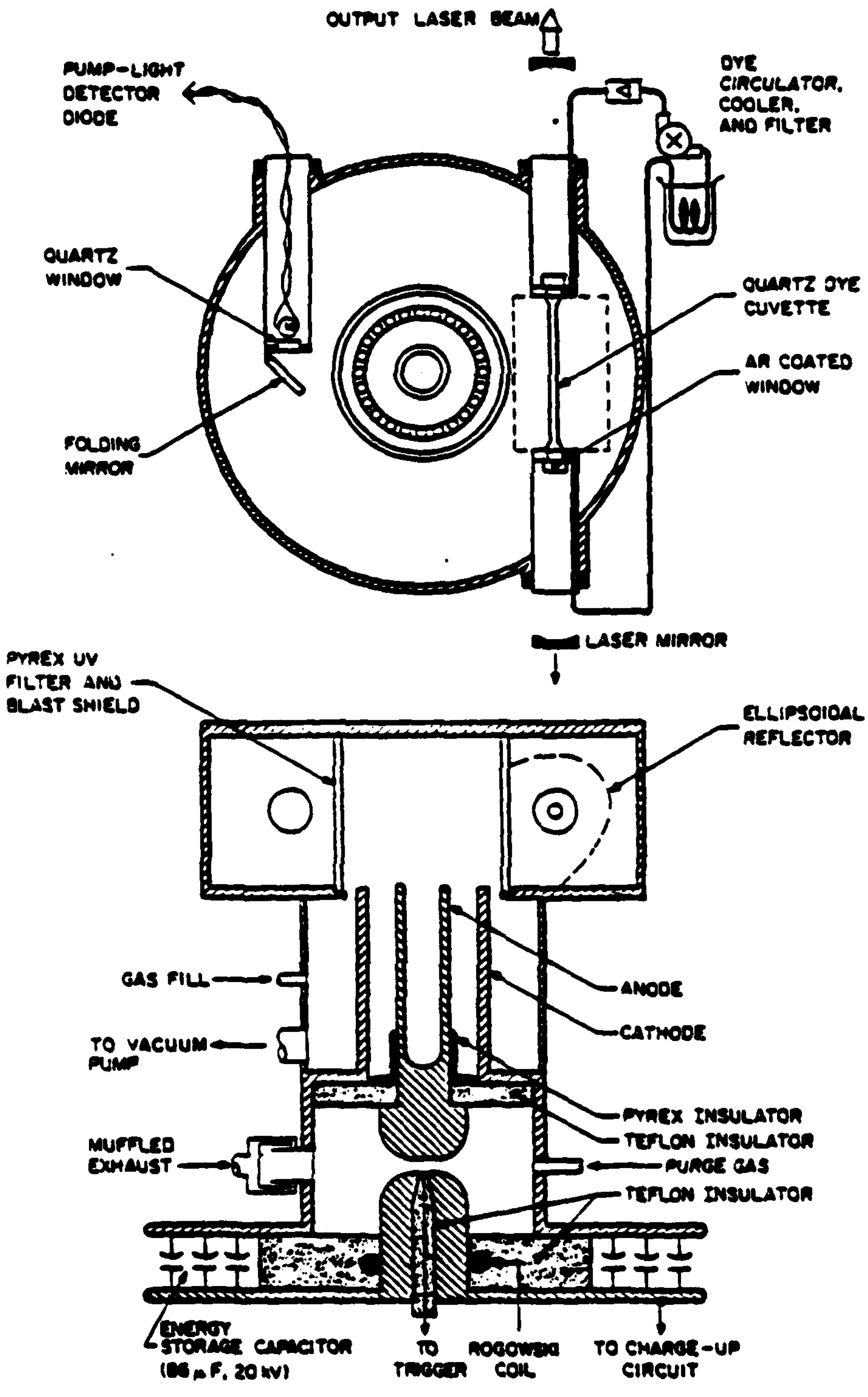

Figure 1. MDPF-Pumped laser apparatus.

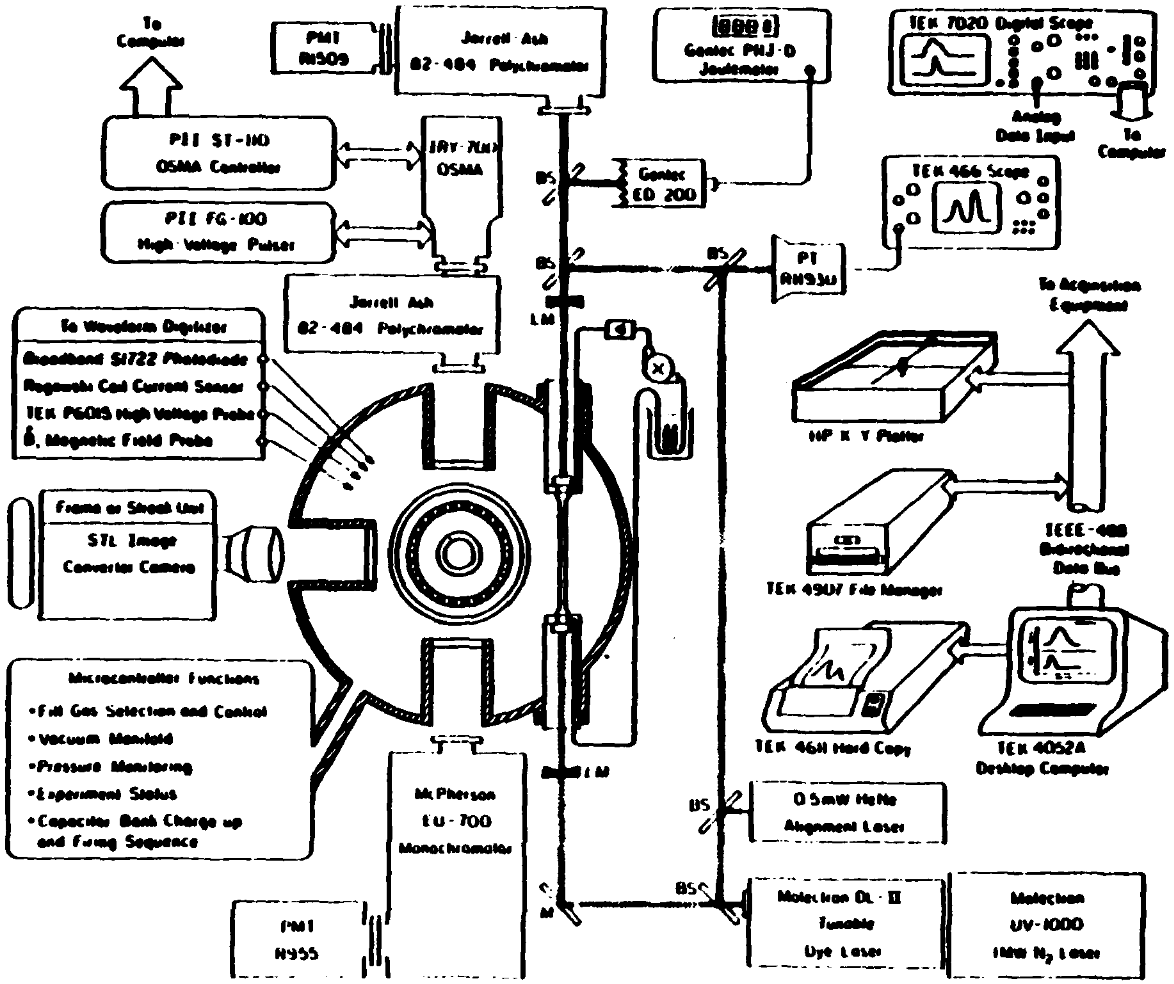

Figure 2. Diagnostic setup for MDPF-laser apparatus.

polychromator with adapters to accept an OSMA intensified head, a Hamamatsu R1509 wide-area photomultiplier tube, or a Polaroid 3 x 5 film pack. To closely follow the plasma current sheet behavior during the focus formation, an STL high-speed framing and streak camera covering 50-, 100-, and 200-ns frame speeds and 5- to 2000-ns streak speeds is used.

Shown in Fig. 3 are the typical electrical and optical signals of the MDPF plasma, which characterize the temporal behavior of the plasma focus formation and the resulting luminescent output. The sudden changes in the signals occurring about 3 μs after the initiation of the plasma current sheet are due to the dense plasma focus formation which momentarily shorts the circuit. The top trace is the capacitor bank voltage, the 2nd and 3rd traces are the plasma current, the 4th one is the anode voltage, and the bottom one is the signal from the plasma light detector diode previously described in conjunction with Fig. 1. This particular set of five traces constitutes a standard diagnostic data set collected for each run and allows one to quickly assess the overall performance quality of each MDPF run. Repeatability of the system performance is also easily judged by comparing the two consecutively obtained sets of traces under the same operating conditions.

The temporal behavior of the MDPF luminescence has been monitored for the selected spectral regions, and is shown in Fig. 4. The top trace shows the time rate of change in the plasma current, and the rest are, respectively, the luminescent output intensities in the regions of 115-165 nm (XUV), 200-300 nm (UV), 300-500 nm (visible), and 500-930 nm (visible to IR). The typical rise time of the optical output is ~200 ns. To compare the total radiant energy output of the MDPF plasma in those four spectral regions, Fig. 4 has been time-integrated. These results are shown in Fig. 5. With this, and knowing the location and size of the photosensors used, we conservatively estimate that about 50% of the input electrical energy is converted into the output optical radiation above 115 nm, and that about 75% of the optical output is

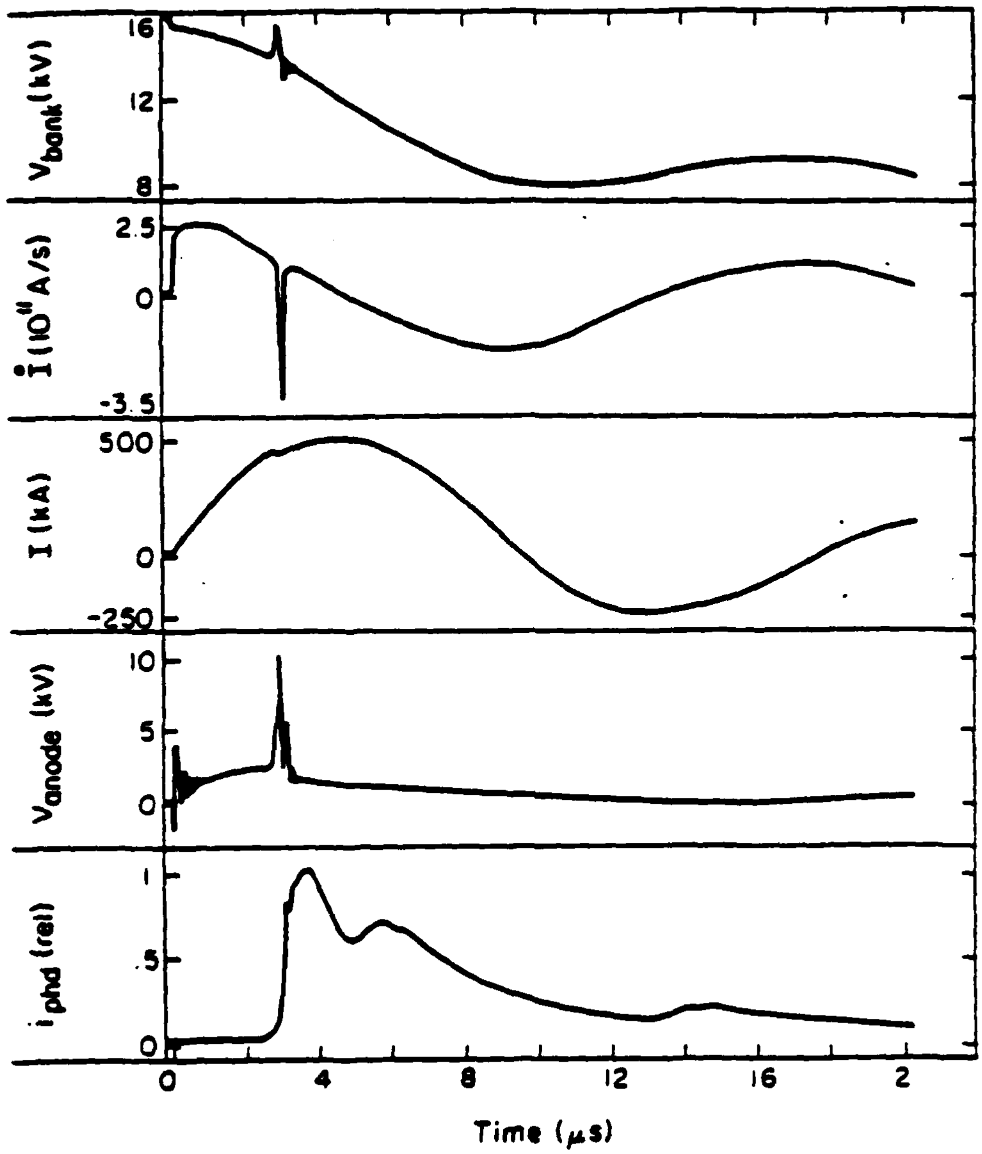

Figure 3. Typical operating characteristics of MDPF.

below 200 nm. In light of the fact that commercial Xe flashlamps have very little optical output in the wavelengths < 200 nm, these preliminary results clearly indicate that the MDPF light source is far superior to the Xe flashlamps as far as the short-wavelength capabilities are concerned.

To assess the feasibility for employing MDPF as a laser optical pump, lasing experiments were performed using the laser cavity setup illustrated in Figs. 1 and 2. Although organic liquid dyes were used as the sample lasing media, it was not out of necessity but rather for the ease of sample selection and low cost. Other lasing media, such as gas and solid materials, can therefore be tested with the same setup with very few alterations. The principal diagnostics employed for this study were a Molectron brand UV-100 1-MW N_2 laser/DL-II tunable dye laser system for the gain measurement and a Gentec brand PRJ-D digital readout joulemeter with ED-100/ED-200 calibrated detectors.

The results of the small signal gain measurements performed on a rhodamine 6G dye solution in 1:1 MeOH:DIH_2O are shown in Fig. 6(a) as a function of the capacitor bank voltage. The maximum observed gain is 23% cm^{-1} which is obtained at the capacitor bank voltage of 18 kV, a hydrogen gas fill of 3 torr, and a dye solution of 5 X 10^{-14}-M/ concentration. The laser output energy is plotted against the capacitor bank voltage for three different values of the output mirror percent transmittance (%T). The highest laser output energy is in the range of 0.5 J, and is obtained at the capacitor bank voltage of 18 kV and the output mirror %T of 30%. The laser output energy is also plotted against the dye concentration and the %T of the output mirror in Fig. 7. It is clear from Figs. 6 and 7 that one can easily increase the laser output energy by increasing the capacitor bank voltage and/or the %T of the output mirror. Also to be noted is the fact that the results contained in Figs. 6(b) and 7 were obtained using a quartz filter as the protection shield between the plasma focus and the laser cavity. With a pyrex filter, as

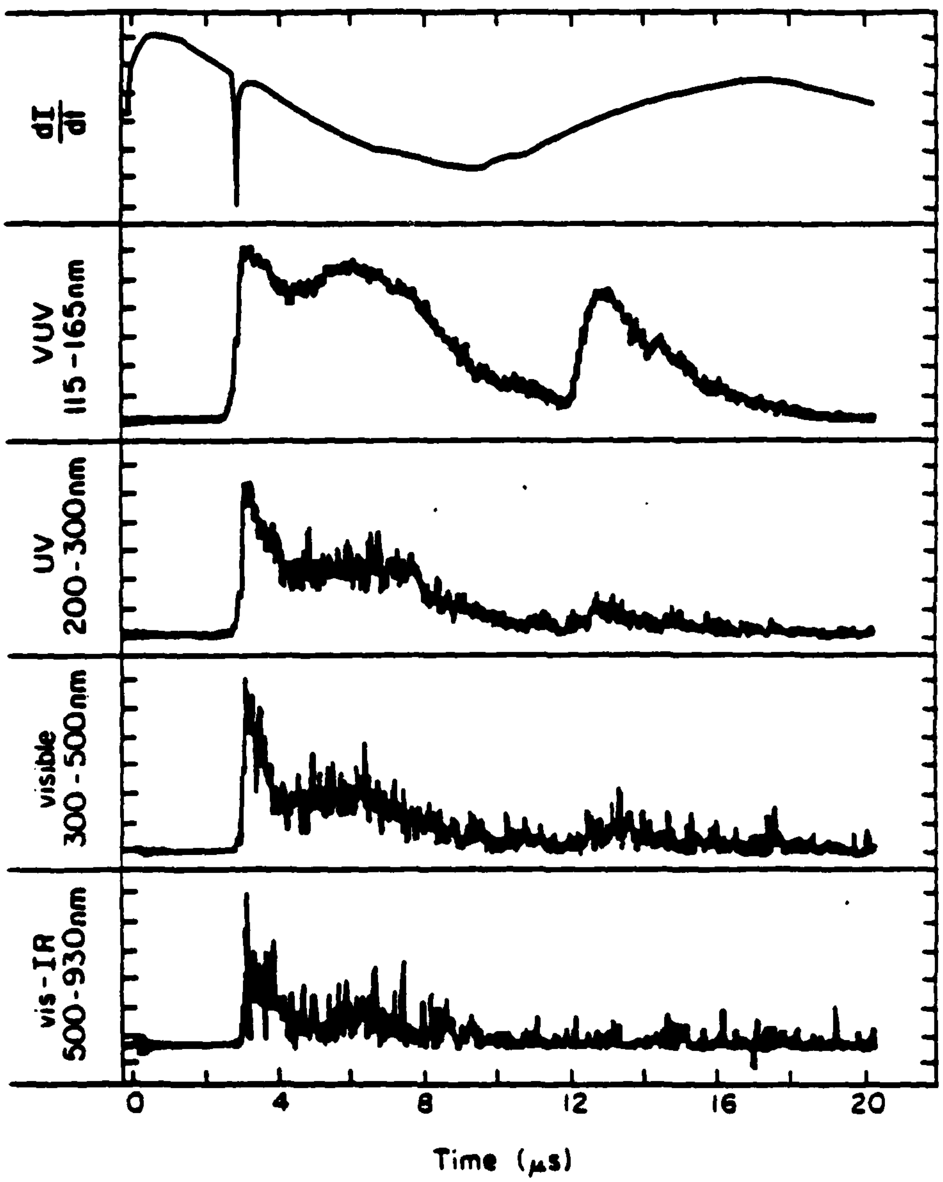

Figure 4. Typical temporal intensity outputs of MDPF for selected wavelength regions.

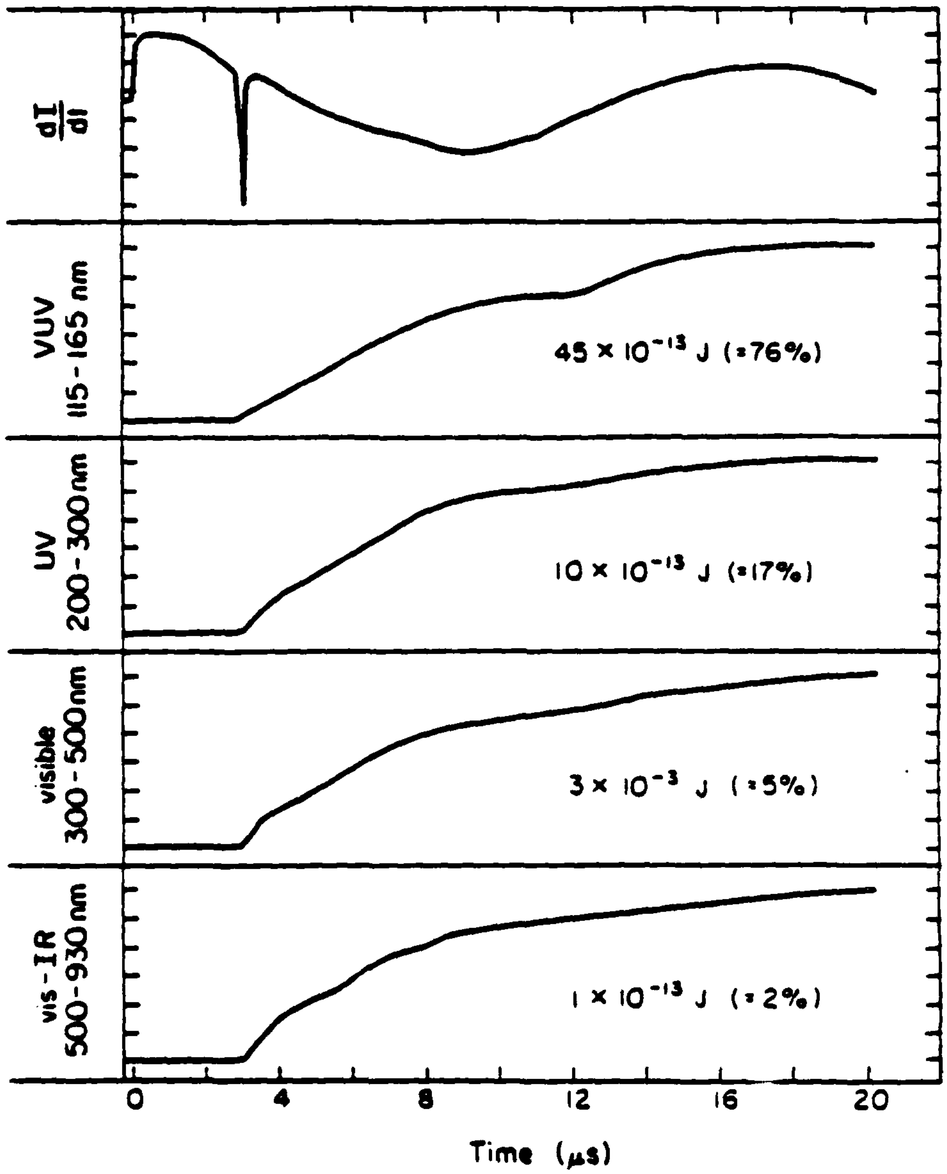

Figure 5. Integrated intensity outputs of MDPF for selected wavelength regions.

expected, the measured values of the laser output energy were somewhat lower, the difference being as much as a factor of 3.

The results for coumarin 480 in MeOH are shown in Fig. 8, which were obtained using a quartz filter as the protection shield. Figure 8(a) is a plot of the laser output energy vs. the dye concentration. It is seen from this figure that the maximum laser energy is slightly over 50 mJ, which occurs when the dye concentration, the hydrogen fill pressure, the capacitor bank voltage, and the output mirror percent transmittance are, respectively, 1×10^{-4} M/ℓ, 3 torr, 18 kV, and 20%. The fact that the laser output energy of coumarin 480 is lower than that of rhodamine 6G by a factor of 10 is not because the MDPF luminescence is low in UV emission but because of the low lasing efficiency of coumarin and a poor overlap between the MDPF luminescence and the coumarin absorption band. Figure 8(b) is the plot of the laser energy vs. the output mirror %T, which indicates that the laser energy will be higher when an output mirror with a greater %T is used. Since such a mirror was not available at the time of the experimentation, higher laser output energy could not be achieved.

Spatially, the evolution of the plasma sheath and ensuing metal vapor emission could be followed using a 50-ns exposure framing camera. The plasma sheath was seen to roll over the top of the electrode structure (Fig. 9a), deflect around the end and remain attached to the inner surface as it collapsed towards the center. A portion of the luminous sheath was seen to break off of the focus and continue to expand outwardly. At the same time, electron bombardment of the anode created an intense radiation emanating from the inside of the anode. Inspection of the anode after many shots indicated strong bombardment of the inside surface extending 2-cm down. The use of a hollow anode (Fig. 9a) is advantageous in that it does obstruct the focus region and should provide the best situation for complete plasma compression. It suffers, however, in that it does not fully utilize the electron beam

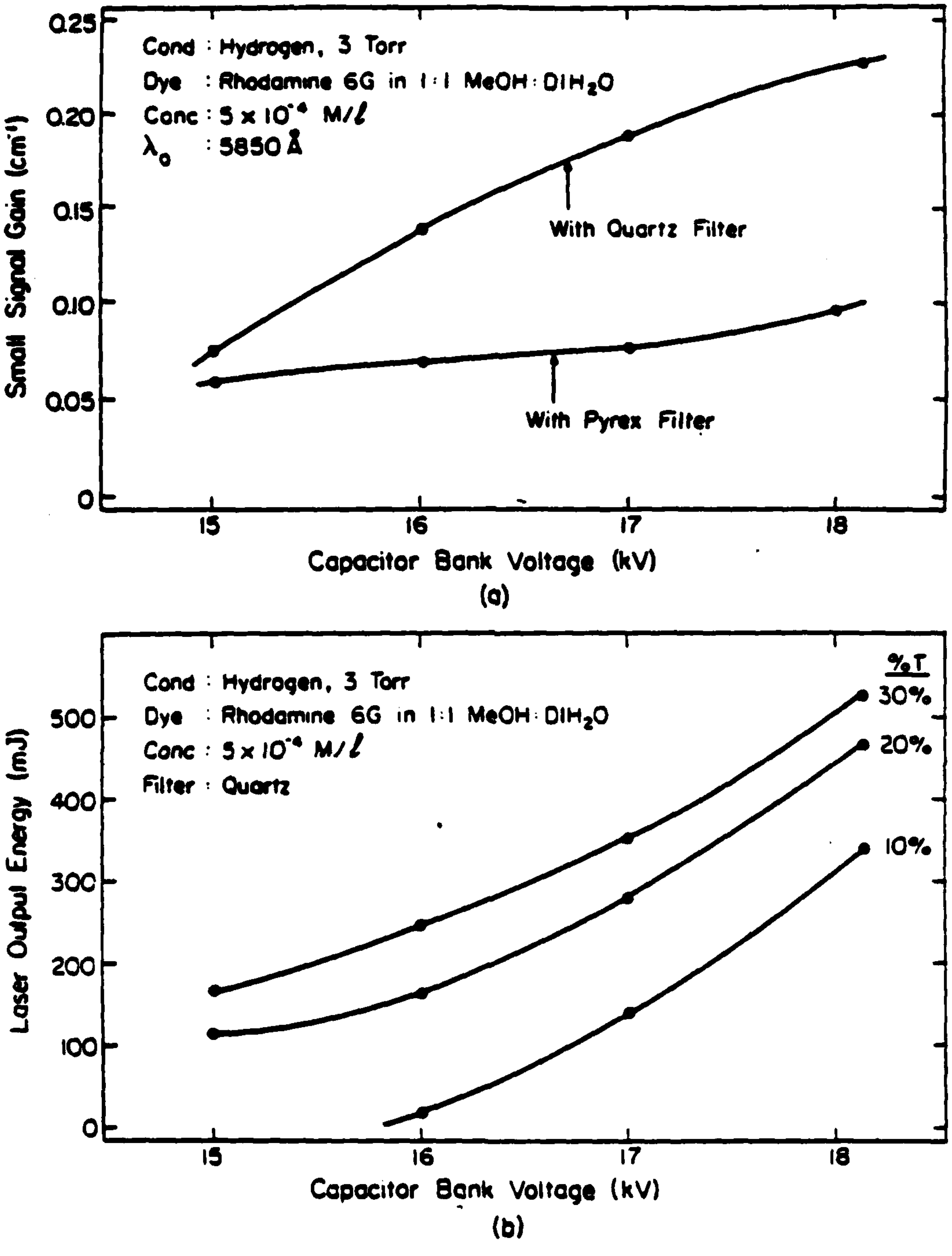

Figure 6. Results of lasing experiment on rhodamine 6G dye.
(a) Small signal gain vs. capacitor bank voltage
(b) Laser output energy vs. capacitor bank voltage

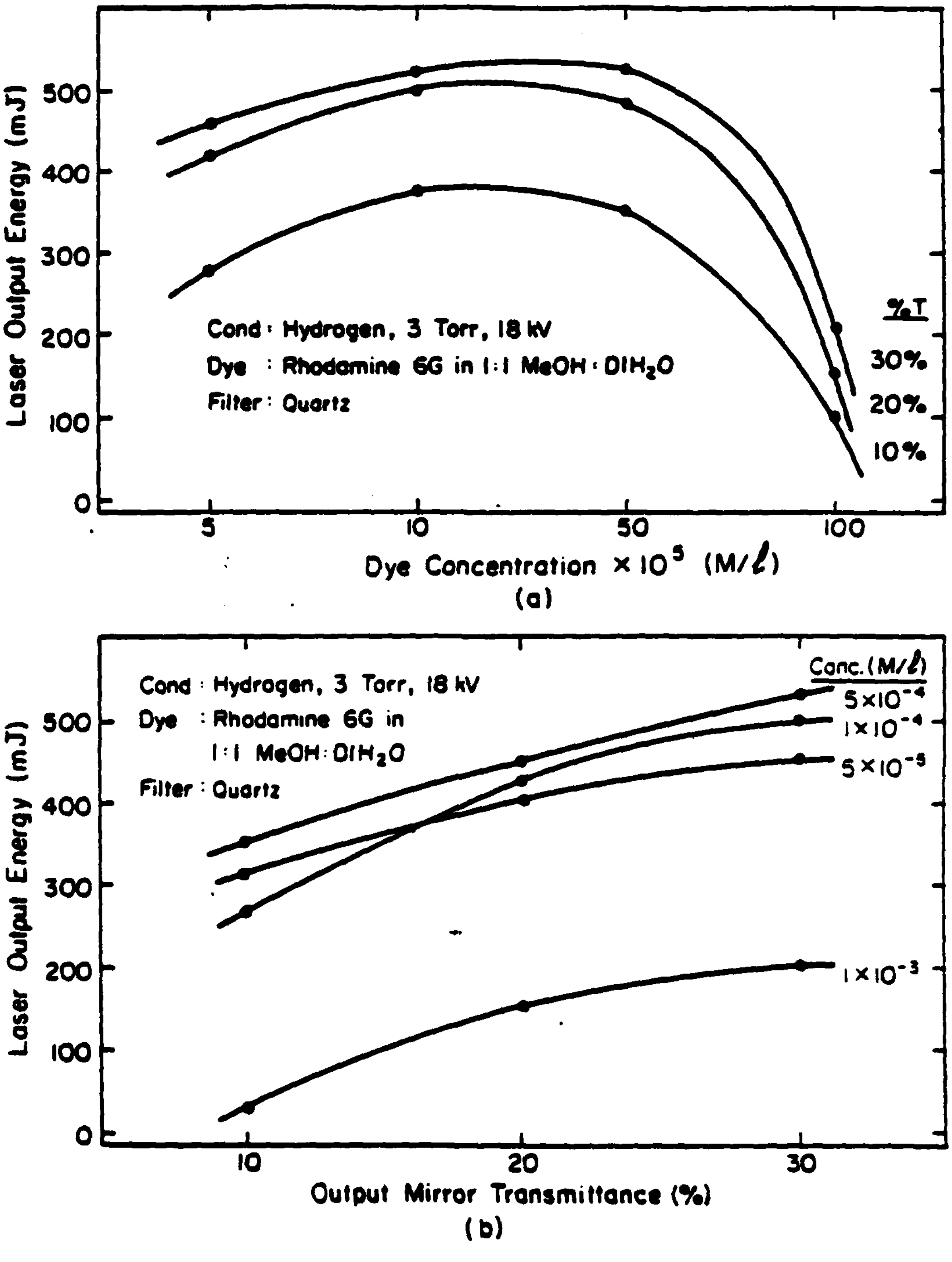

Figure 7. Results of lasing experiment on rhodamine 6G dye.
(a) Laser output energy vs. dye concentration
(b) Laser output energy vs. output mirror transmittance

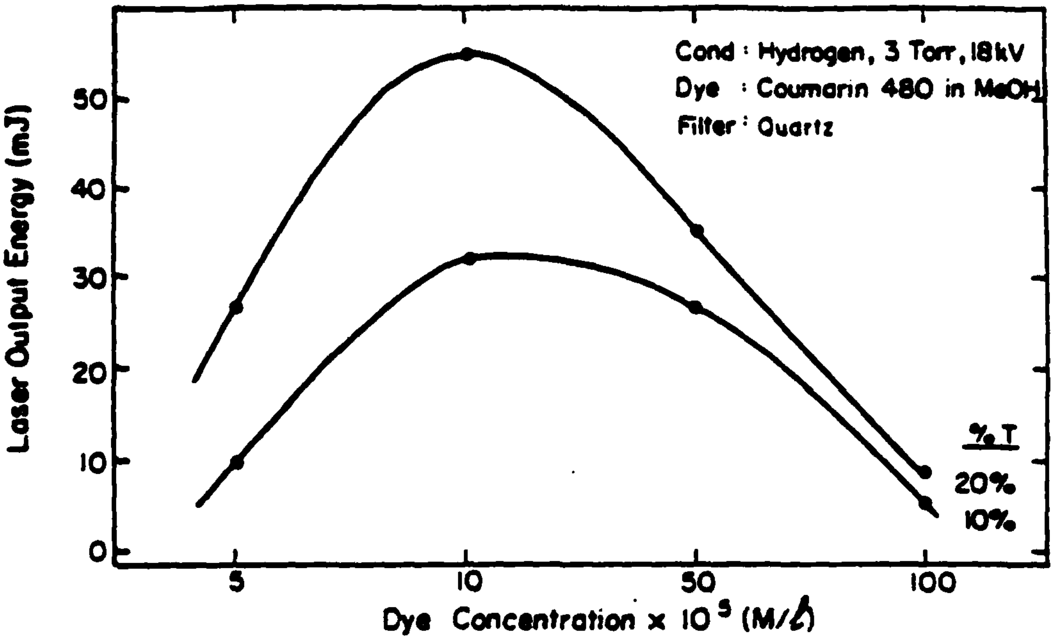

(a)

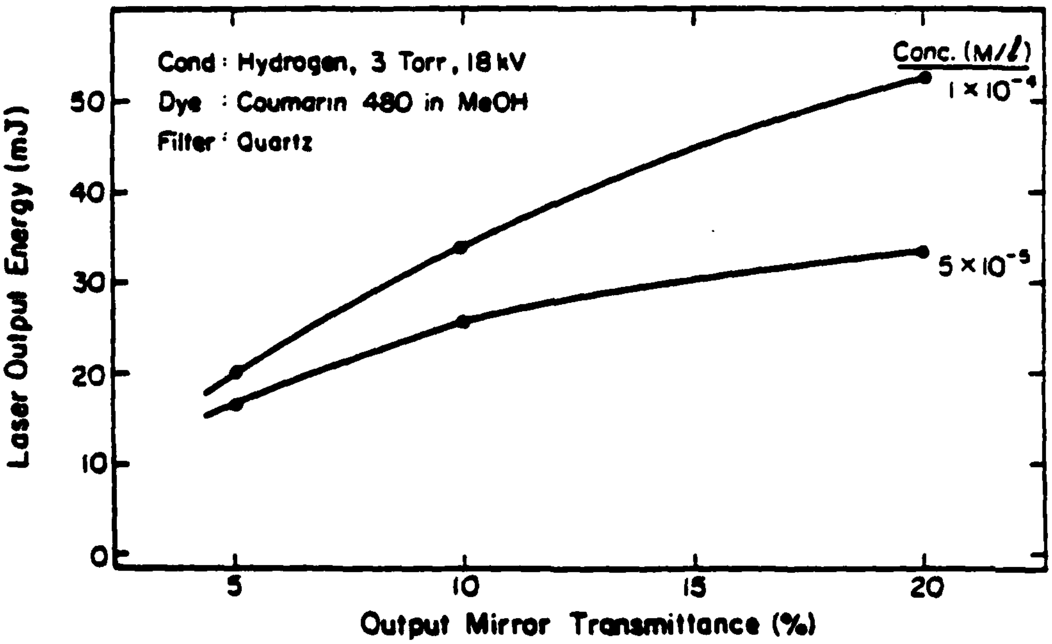

(b)

Figure 8. Results of lasing experiment on coumarin.
(a) Laser output energy vs. dye concentration
(b) Laser output energy vs. output mirror transmittance

generated in the focus for production of radiation.

The use of a completely solid anode, as shown in Fig. 9b, greatly increased the metal vapor emission. The solid electrode, however, created a drag force on the sheath and interfered with the pinch phase. Presence of a small dimple at the center (Fig. 9c) enhanced the radiative output by allowing a good focalization and thus electron beam formation.

The next experiment used a copper target placed in the focal region as shown in Fig. 9d. The presence of the target caused a double pinch to occur. The first focus was situated about the base of the target. The usual sequence of axial wave and shock front movement occurred. In addition, the current sheath was seen to propagate up the target and collapse again on top. At this point, the usual electron beam bombardment took place and an additional metal vapor plasma was produced. The results indicated that the spatial characteristics of the plasma may be controlled by proper anode design. For example, an IC exposure imaging system would require a compact radiation point source, which could be obtained by an anode moderately tapered to a small cylindrical target.

In the case of laser pumping, the radiation source should be rather large and isotropic. An optimal design would involve the noninterfering aspects of a hollow anode (Fig. 9a) and the optimized radiation effects of using a direct beam target (Fig. 9b). For this work, the best anode design was a shallow concave depression with a high Z-target material at its center.

Experiments were also performed to measure the output radiated by the metal vapor resulting from a variety of electrode materials. Figure 10 represents the effect of Z on radiated output. Each spectrum was taken at peak intensity of the focus. The given material was placed in a solid anode structure and was directly bombarded by the electron beam. The Z-dependence of the spectral emission is clearly shown by the scarce line radiation in the low-Z aluminum target in comparison to the broad continuum seen in the high-Z

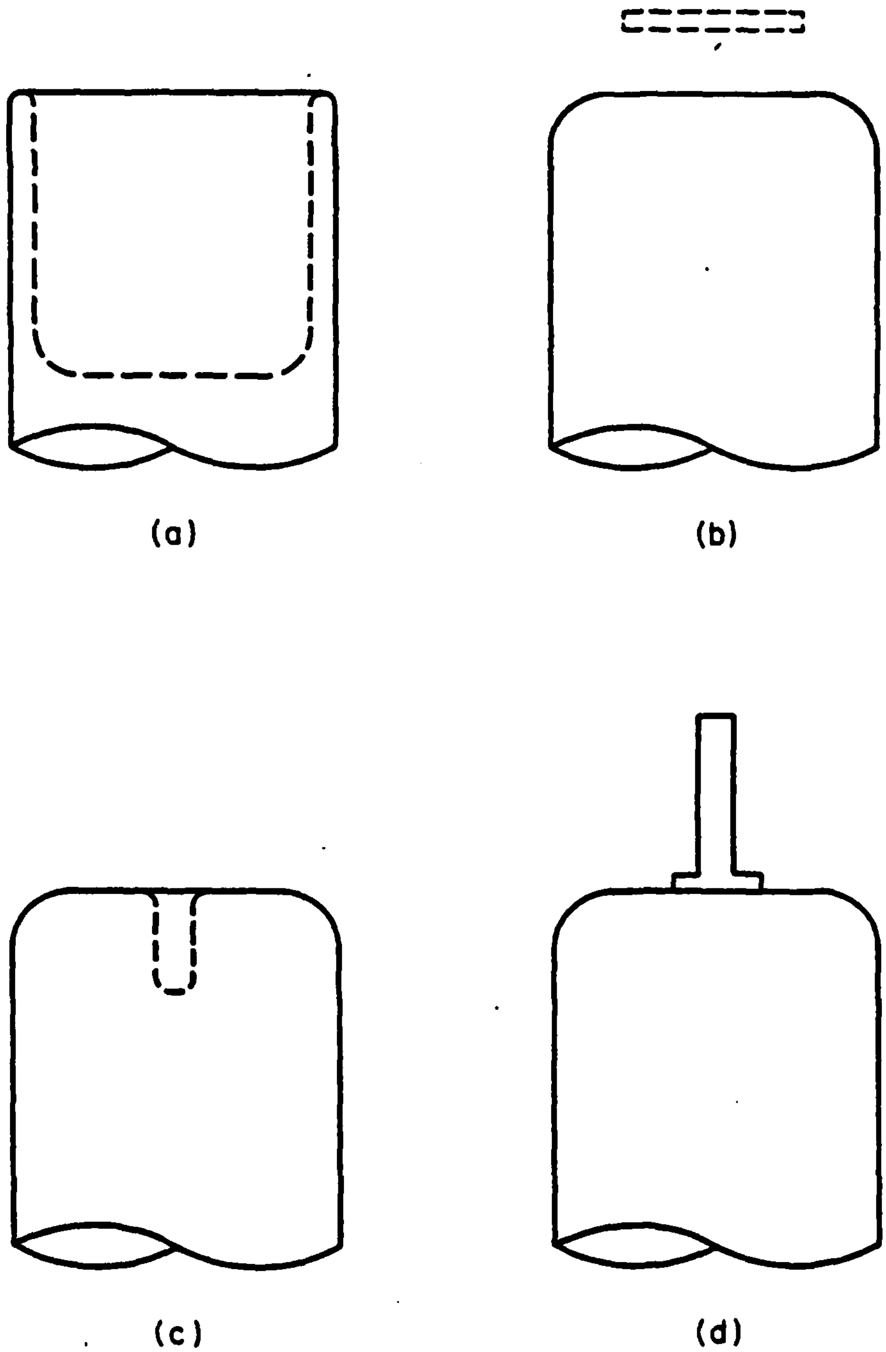

Figure 9. Anode configurations.
(a) Hollow
(b) Solid
(c) Solid with dimple
(d) Solid with target

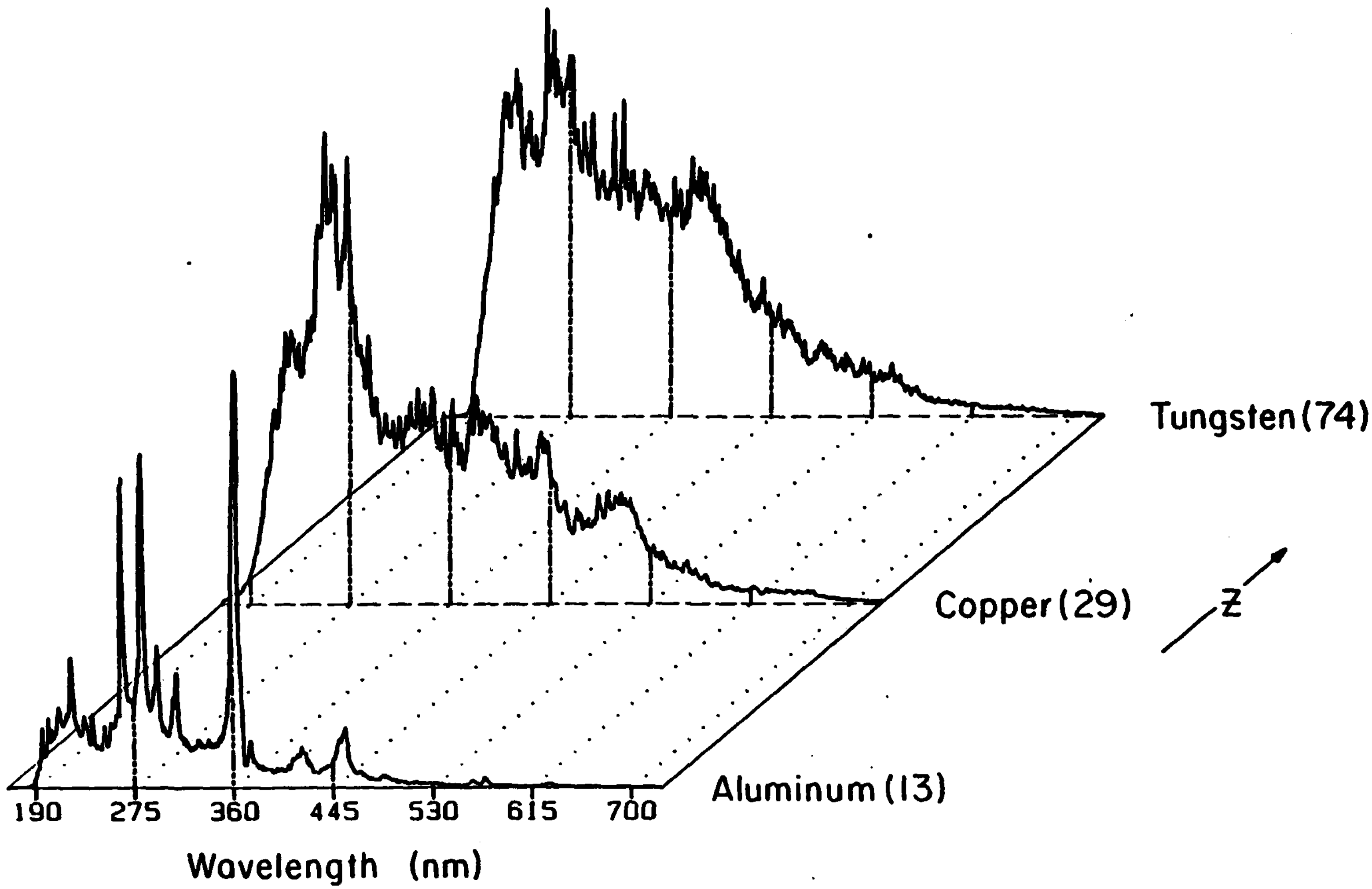

Figure 10. Spectral results for various beam-target materials.

tungsten target. The roll-off at 200 nm is due to the response of the OSMA system. The spectrum represents only the tail of the continuum that peaks in the VUV region. The results clearly indicate the necessity of using high-Z materials for production of broadband emission.

C. References

1. P.P. Sorokin and J.R. Lankard, IBM J. Res. Develop. 10, 162 (1966).
2. W. Schmidt and F.P. Schafer, Z. Naturforsch. 22a, 1563 (1967).
3. P. Gensel, K.L. Kompa, and J. Wanner, Chem. Phys. Lett. 1, 583 (1970).
4. H.W. Furumoto and H.L. Ceccon, IEEE J. Quant. Electron. QE-6, 262 (1970).
5. V.A. Alekseev, I.V. Antonov, V.E. Korobov, S.A. Mikhnov, V.S. Prokudin, and B.V. Skvortsov, Sov. J. Quant. Electron. 1, 643 (1972).
6. V.A. Alekseev, N.P. Kozlov, and Yu.S. Protasov, Instruments and Experimental Techniques 16, 1774 (1973).
7. C.M. Ferrar, Appl. Phys. Lett. 23, 548 (1973).
8. C.M. Ferrar, Optica Acta 23, 911 (1976).
9. W.T. Silvast and O.R. Wood II, Appl. Phys. Lett. 26, 447 (1975).
10. B.L. Borovich, V.S. Zuev, V.A. Katulin, V.Yu. Nosach, O.Yu. Nosach, A.V. Startsev, and Yu.Yu. Stoilov, Sov. J. Quant. Electron. 5, 695 (1975).
11. A.V. Antonov, N.G. Basov, V.S. Zuev, V.A. Katulin, K.S. Korol'kov, G.V. Mikhailov, V.N. Netemin, F.A. Nikolaev, V.Yu. Nosach, A.L. Petrov, and A.V. Shelobolin, Sov. J. Quant. Electron. 5, 123 (1975).
12. M.A. Gusinow, IEEE J. Quant. Electron. QE-11, 929 (1975).
13. M.A. Gusinow, J. Appl. Phys. 46, 4847 (1975).
14. M.A. Gusinow, Appl. Opt. 14, 2645 (1975).
15. R.T. Brown, IEEE J. Quant. Electron. QE-11, 800 (1975).
16. N.P. Kozlov, A.S. Kamrukov, G.N. Kashnikov, V.A. Malashchenko, V.K.

Orlov, and Yu.S. Protasov, Sov. Tech. Phys. Lett. 1, 196 (1975).

17. N.P. Kozlov and Yu.S. Protasov, Sov. Phys. Dokl. 20, 500 (1975).

18. A.S. Kamrukov, G.N. Kashnikov, N.P. Kozlov, V.A. Malashchenko, V.K. Orlov, and Yu.S. Protasov, Sov. J. Quant. Electron. 6, 1101 (1976).

19. R.E. Beverly III, R.H. Barnes, C.E. Moeller, and M.C. Wong, Appl. Opt. 16, 1572 (1977).

20. J.C. Swingle, C.E. Turner, Jr., J.R. Murray, E.V. George, and W.F. Krupke, Appl. Phys. Lett. 28, 387 (1976).

21. J.H. Lee, D.R. McFarland, and F. Hohl, Appl. Opt. 19, 3343 (1980).

22. H. Rieger and K. Kim, J. Appl. Phys. 52, 5381 (1981).

23. N.V. Filippov, T.I. Filippova, and V.P. Vinogradov, Nucl. Fusion Suppl. Pt. 2, 577 (1962).

24. J.W. Mather, Phys. Fluids Suppl. 7, 5 (1964).

25. K. Kim and J.J. Fanning, Proc. Conference on Lasers and Electro-Optics, Anaheim, California, June 1984.

26. A review article by J.W. Mather in Methods of Experimental Physics, vol. 9, Part B (Academic Press, New York, 1971), p. 187.

III. CONCLUSIONS

For the first time, successful operation of an MDPF as an optical pump source for lasers was achieved. The preliminary experiments involved optical excitation of organic liquid dyes. In a proof-of-principle setup the MDPF was capable of generating a laser energy density of 225 mJ/cm^3 for rhodamine 6G. Further results indicated that the focus is an efficient source of VUV-to-visible radiation for short-wavelength laser pumping and UV microlithography. Experiments with energy scaling indicated a superlinear relationship between increases in electrical input energy and the resultant optical or laser output energies.

The dominant radiation mechanism in the MDPF is the electron bombardment of the anode. The bombardment process creates an isotropic hemispherical radiation pattern. Proper design of the anode cap is vital in optimizing the radiated output. Results indicated that a smooth concave depression in a high Z material, such as tungsten or tantalum, will produce the greatest optical power output. To utilize all of the available light, the laser cavity should encompass the entire periphery outside the MDPF electrode structure. Efficient collection of the radiated output should be assured by using reflectors capable of imaging the metal plasma source onto the properly sized dye cuvettes. A 4-arm setup with reflectors is capable of intercepting approximately 85% of the available MDPF-radiated output.

The 4-arm configuration includes a novel approach for utilizing the broad tunability characteristics of laser dyes. One arm can be used as a narrow-band tunable master oscillator operating at low power levels. The output of the oscillator is then injected into a high-gain 3-arm amplifier. The master-slave combination provides a compact method of achieving a high-power tunable laser.

The 4-arm capability of the MDPF may also be configured as four separate laser oscillators. In this case, it is possible to use four different dyes, or possibly, solid-state rods to achieve four simultaneous discrete-wavelength emissions. The broadband spectral output of the MDPF would provide adequate pumping power throughout the VUV-to-visible wavelength regions.

With regards to optimizing the temporal lasing characteristics of organic dyes, several detrimental effects must be overcome. All the experimental lasing results showed a premature termination of laser activity, thus under-utilizing the long-pulse capabilities of the MDPF. Short-term disruption in the lasing process is due to triplet-quenching effects. These effects may be controlled by use of commercially available additives. Long-term disruptive effects are due to thermal instabilities in the dye solution. Thermal stability may be achieved by use of a very fast dye circulation system, high-heat capacity solvents, and optical filters that block out any unusable radiation components outside the absorption band of the dye.

Temporal optimization also includes increasing the risetime of the pumplight pulse. This will inherently improve laser operating efficiency by creating a faster initial inversion, thus achieving threshold levels sooner and minimizing energy lost to non-lasing relaxation processes. A faster rise time system would be capable of lasing a greater number of laser media, particularly the short-wavelength-emitting dyes.

The intense UV radiation of the MDPF can lead to accelerated dye degradation by molecular chain scission. Again, a UV-blocking filter can be used, as was done with pyrex glass in the rhodamine 6G experiment. Since the rhodamine 6G does have some useful absorption in the UV, however, elimination of the UV pump light strongly decreased the laser output energy. Without the UV filter, use of a large-capacity reservoir and fast circulation system would minimize the degradation effects.

Another possibility for utilizing the strong UV emission of the MDPF

would involve the use of several dyes. A shorter wavelength dye could be used to absorb the high energy photons and subsequently fluoresce at longer wavelengths corresponding to the absorption band of the longer wavelength-emitting dye.

It was previously thought that the MDPF-radiated output could be tuned specifically to the absorption band of the given laser media. Experimental results of the DPF with different fill gasses and pressures, anode materials, and operating energies indicated that only a minimal selectivity in spectral output is possible.

Use of different fill gasses generally resulted in decreased MDPF performance. To obtain the same effective mass density, operating the MDPF with higher-atomic-weight gasses requires lowering the operating pressure accordingly. It was found, however, that operation at the same gas mass density with different type gasses did not give similar results. Typically, the amplitude of the dI/dt current spike was noticeably less than when hydrogen was used. The amplitude of the spike is an indication of effective compression in the pinch phase. Poor performance in the pinch phase results in a less-effective electron beam generation. This, in turn, leads to a lower metal vapor emission and decreases radiated energy output. Generally, for a given gas species only one particular fill pressure will give optimal MDPF performance.

The spectral-line emission output from the different gas species is completely obscured by the continuum of the metal vapor when high-Z beam targets are used. As a result, the use of different gas species and fill pressures is not an effective means of controlling the spectral output of the MDPF. Best operating results are obtained using hydrogen gas at 2 to 3 Torr fill pressures.

Other possibilities for tuning the output spectrum of the MDPF require use of different target materials on the top of the anode. The radiated

output from the hot and dense metal vapor of the target creates line, recombination, and Bremsstrahlung emissions. As the atomic weight of the target material is increased, the emitted power by the highly-broadened line emissions increases by Z^6, the recombination emission increases by Z^4 and the Bremsstrahlung emission increases by Z^2. For a high-Z target, the output spectrum becomes very dense and appears as a smooth continuum throughout the UV-to-visible wavelength region (see Fig. 10). In addition, the use of high-Z target materials produces the best total radiated output energy.

Although it is possible to obtain different line spectra by use of different low-Z materials, the drastic decrease in overall radiated energy will always reduce the operating coupling efficiency. For a high-Z target, variation in operating energies has shown little shift in the UV-to-visible spectral range. Increasing the electron beam current and energy by increasing the DPF operating energy will cause a shift in the peak of the continuum emission. The shift in the peak, however, is deep in the VUV (5-10 eV) and measurements in the UV-visible range simply show an increase in radiated power with little change in the spectral content.

In summary, best results are obtained with a properly designed anode constructed out of high-Z material and 2-3 Torr hydrogen gas. The resultant spectrum is a very broad continuum extending from deep in the VUV to approximately 550 nm. Although spectral tuning is limited, the broadband nature of this source will encompass many existing ultra-short to visible wavelength laser media.

Electrical optimization of the MDPF relies on the energy bank's ability to deliver the highest possible current in the shortest period of time with little or no energy wasted. The current dependence is due to the fact that the final peak compression relies on the strength of the confining magnetic field which depends on the square of the discharge current. In order to maximize the current into the DPF discharge, the bank impedance

$Z_B=(L_E/C_B)^{1/2}+R_E$ should be maximized. Typically, C_B is determined by the prescribed operating energy ($CV_o^2/2$) and L_E is usually made as low as possible to obtain high rates of current change. The final result is a low impedance of the bank whose current flow and current efficiency are greatly affected by the time-varying inductance of the MDPF.

Remarkable improvements have been made by Decker et al., 1983, with the development of their SPEED1 focus device. The device has a bank impedance of 160 m , initial current rise of $>5X10^{12}$ A/s, a current efficiency of 30 A/J, and a current derivative spike of $>10^{13}$ A/s (FWHM 10 ns). The system only has a breakdown and collapse phase and reaches final compression in under 500 ns. This is an order of magnitude improvement in speed over the devices used in this study! The disadvantage of the setup is that it operates at 120 kV. Some of the techniques applied here, however, can be implemented in more practical devices.

One of the most outstanding results of the present study was the successful first-time operation of an MDPF at 5 kV. The success was largely due to the improved breakdown performance, which was effected by addition of a knife edge to the cathode structure. Low-voltage MDPF operation permits development of a compact, reliable solid-state switched focus capable of high rep rates.

To alleviate the additional leakage current created by the knife edge, a pulsed preionizer may be used. The preionizer would provide an ample initial source of free electrons for breakdown and retain the insulating integrity of the breech during the rundown and collapse phases.

During the course of the investigation of the MDPF as an optical pump source for lasers, it became obvious that the focus can provide an ideal source of high-intensity radiation for soft X-ray and VUV microlithography. The intense VUV radiation, which is the predominant optical energy output of the DPF, may be used in conjunction with MgF_2 optics to produce micron- and

submicron-sized geometries on integrated circuits. Even finer detailed geometries may be achieved by making use of the DPF's abundant source of soft X-rays.

END
10-86
DTIC